1 Heterostructure materials

It is as easy to count atomies, as to resolve the propositions of a lover.

As You Like It, WILLIAM SHAKESPEARE

1.1 Introduction

Modern growth technologies have made possible the growth of new semiconductor devices with unprecedented control on the atomic level. In this chapter we shall briefly introduce the molecular beam epitaxy (MBE) growth technique and discuss its application to the growth of materials (alloys, pseudomorphic, modulation doped) for new device structures. The chapter will conclude with a review of the cubic crystal structure and its reciprocal lattice, as these concepts are used extensively in Chapters 2 and 3.

1.2 MBE technology

One of the most versatile growth techniques available for research is the MBE. In this growth technique a semiconductor substrate is placed in a high-vacuum chamber (see Figure 1.1). Different components such as Ga, Al, As, In, P, and Si are heated in separate closed cylindrical cells. These components escape through an opening in the cylindrical cell and form a molecular beam. These beams are directed toward the substrate. A shutter positioned in front of each cell is used to select the desired molecular beams. By selecting a low temperature for the substrate growth and a slow growth rate (a few micrometers per hour), it is possible to grow high-quality crystals, while making abrupt changes in doping and crystal composition.

This growth technique can be used to grow semiconductor alloys such as $Al_xGa_{1-x}As$, $In_xGa_{1-x}As$, $In_xAl_{1-x}As$, and $Si_{1-x}Ge_x$, where x, the mole fraction, specifies the composition of the alloy. For example in $Al_xGa_{1-x}As$, Al and Ga are randomly distributed over the same Ga lattice site of the GaAs crystal and x gives the fraction of Ga sites occupied by Al.

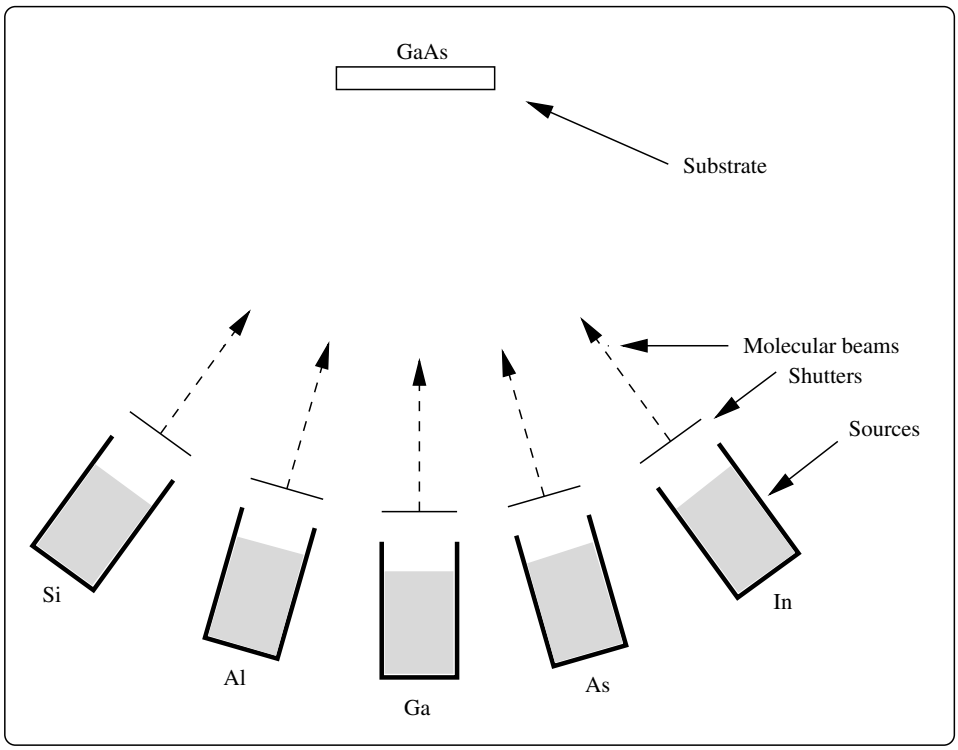

Fig. 1.1. Simplified diagram of an MBE growth chamber.

1.2.1 Lattice-matched systems

The epitaxial growth of one semiconductor on top of another requires that they have a similar lattice parameter so as to minimize the number of defects in the epitaxial layer. As can be seen in Table 1.1, Ge, GaAs, and AlAs have nearly the same lattice parameters. The lattice mismatch measured as $\Delta a/a$ is a fraction of 1%, and these semiconductors can be grown epitaxially on top of each other with extremely small concentrations of defects. This is therefore also the case of the alloy $Al_xGa_{1-x}As$. Complex heterostructures making use of the bandgap variation between the GaAs and AlAs bandgaps can then be grown on a binary GaAs substrate as is illustrated in Figure 1.2.

The $Al_xGa_{1-x}As$ and Ge system is, however, an exceptional case. For example GaAs, InAs, and their alloy $In_xGa_{1-x}As$ can be seen in Figure 1.2 to have quite different lattice parameters leading to a lattice mismatch of up to 7%. In such a case the growth of lattice-matched semiconductor alloys can be achieved by selecting the mole fraction such that both semiconductor alloys have the same lattice parameter. From Figure 1.2 one can verify that $In_xGa_{1-x}As$ and $In_xAl_{1-x}As$ can be grown epitaxially

Table 1.1. *Material parameters for Ge, GaAs and AlAs.*

	$a(\bar{A})$	$\frac{\Delta a}{a_{GaAs}}$	E_g	χ (affinity)
Ge	5.6461	1.3×10^{-3}	0.663	4.13
GaAs	5.6533	0	1.424	4.07
AlAs	5.6614	1.2×10^{-3}	2.16	3.5

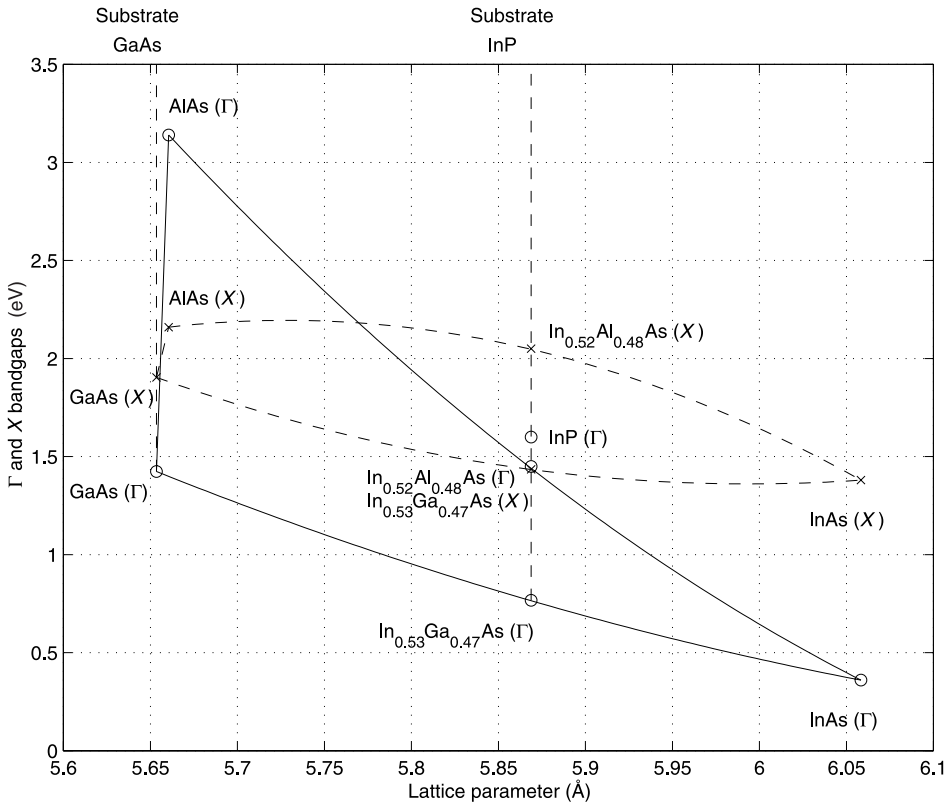

Fig. 1.2. Direct (optical) Γ (plain line) and indirect X (dashed line) bandgaps (see Figure 2.1 for a definition) of the alloys of the semiconductor binaries GaAs, AlAs, and InAs, plotted versus their lattice parameters for all mole fractions x.

on an InP substrate when using the In mole fractions $x = 0.53$ and $x = 0.52$, respectively.

1.2.2 Pseudomorphic materials

The MBE growth technique also permits one to grow lattice-mismatched alloys if the mismatch is only a few percent and the layer is thin. The epitaxial layer grown will

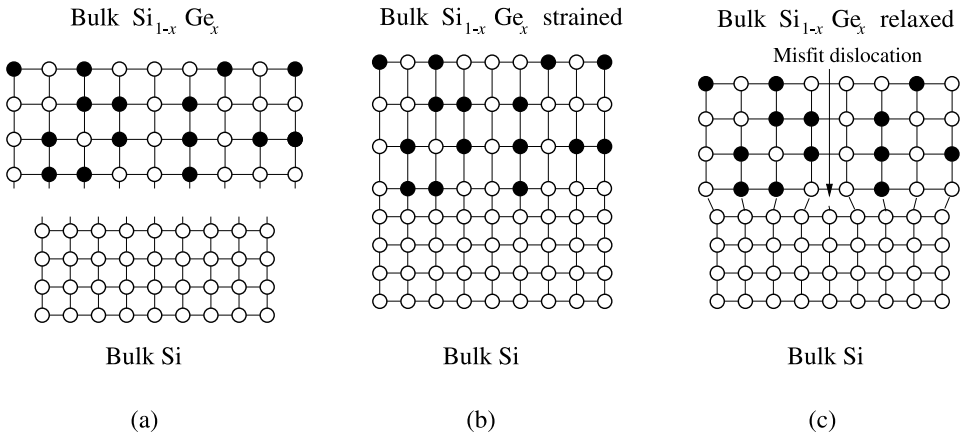

Fig. 1.3. Conceptual formation (a) of a strained pseudomorphic layer (b) and its relaxation (c) for a large thickness.

then assume the lattice constant of the substrate semiconductor on which it is grown. The resulting epitaxial layer is therefore subject to a strain (compression if its natural lattice parameter is larger than that of the substrate or tension if it is smaller) which modifies its physical properties. Such a layer is called pseudomorphic as it assumes a new crystal structure. One can verify, for example, that if the lattice parameter of the epitaxial layer parallel to the interface is reduced, then the transversal lattice parameter is increased as is shown in Figure 1.3(b) in which $Si_{1-x}Ge_x$ is grown on Si.

A pseudomorphic material can only be formed if the epitaxial film thickness is smaller than a critical thickness h_c. This critical thickness corresponds to the thickness at which it becomes energetically more favorable for the epitaxial layer to generate dislocations than to maintain the lattice strain [2]. Figure 1.4 shows the critical thickness for growing $Si_{1-x}Ge_x$ on Si as a function of the Ge mole fraction x. Note that thicker defect-free $Si_{1-x}Ge_x$ films can be grown at a lower growth temperature [3], but these films are metastable and require appropriate subsequent thermal treatments [4].

Other examples of pseudomorphic material systems are $In_xGa_{1-x}As$ and $In_xAl_{1-x}As$ on GaAs and InP substrates and $Al_xGa_{1-x}N$ on GaN. For example $In_{0.25}Ga_{0.75}As$ can be grown for a thickness up to 124 Å on GaAs. For pseudomorphic films of thickness larger than the critical thickness h_c, the film relaxes to its original unstrained bulk lattice, and dislocations are formed, usually rendering the material unusable for making devices.

Pseudomorphic layers can present much improved physical properties. Consider the light- and heavy-hole band structures in Figure 1.5 [1]. In the absence of strain the heavy-hole band is populated due to its higher density of states, and the holes typically exhibit an effective mass much larger than that of electrons. The presence of strain breaks the degeneracy of the light- and heavy-hole bands (see Figure 1.5)

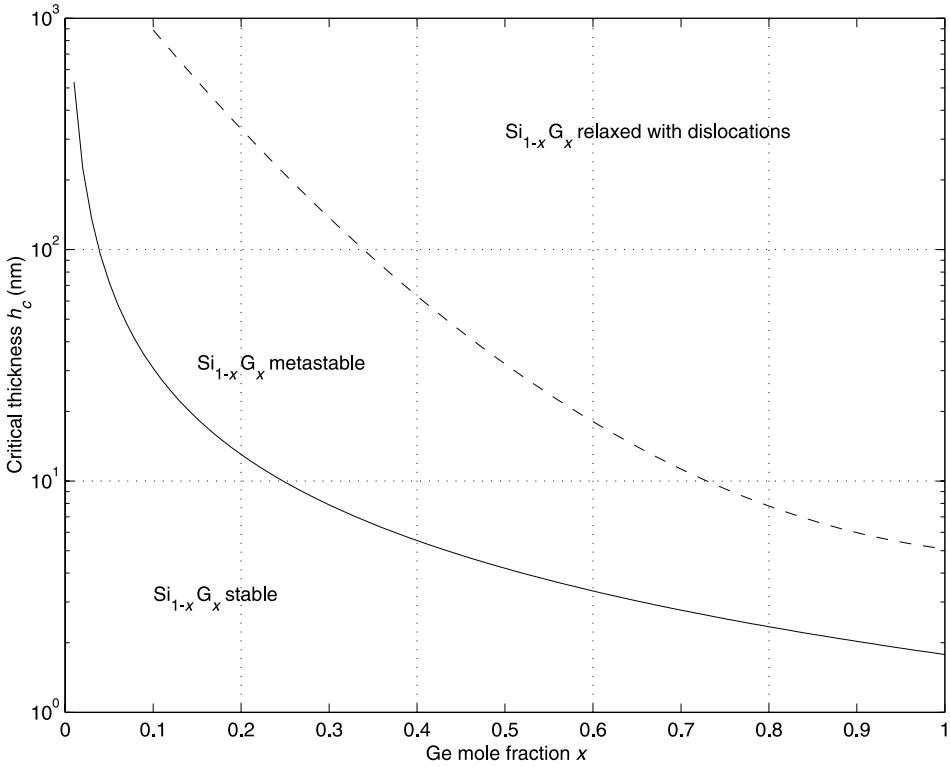

Fig. 1.4. Approximate critical thickness for strained pseudomorphic (full line) and metastable (dashed line) layer in $Si_{1-x}Ge_x$.

at the top of the valence band. When the light-hole band is raised, the light-hole band is preferentially populated, and a high hole mobility results, due to the smaller effective mass of the light holes. In $Si_{1-x}Ge_x$ the heavy-hole mass can even become smaller than the light-hole mass. Pseudomorphic field-effect transistors (FETs) are therefore potentially important for the generation of high-speed complementary logic with p-channel FETs of improved performance.

Other interesting physics can also occur in pseudomorphic materials. For example the large strain present at the interface of $Al_xGa_{1-x}N$ and GaN can, via the piezoelectric effect, enhance the electron charge density.

1.2.3 The materials game and bandgap engineering

Since each semiconductor alloy has a different bandgap (see Figure 1.2) novel heterostructure semiconductor devices can be created using either lattice-matched or pseudomorphic semiconductor epitaxial layers. The most important examples include the semiconductor laser diodes, the heterostructure field-effect transistors (HFETs), the heterojunction bipolar transistors (HBTs), and the resonant tunneling

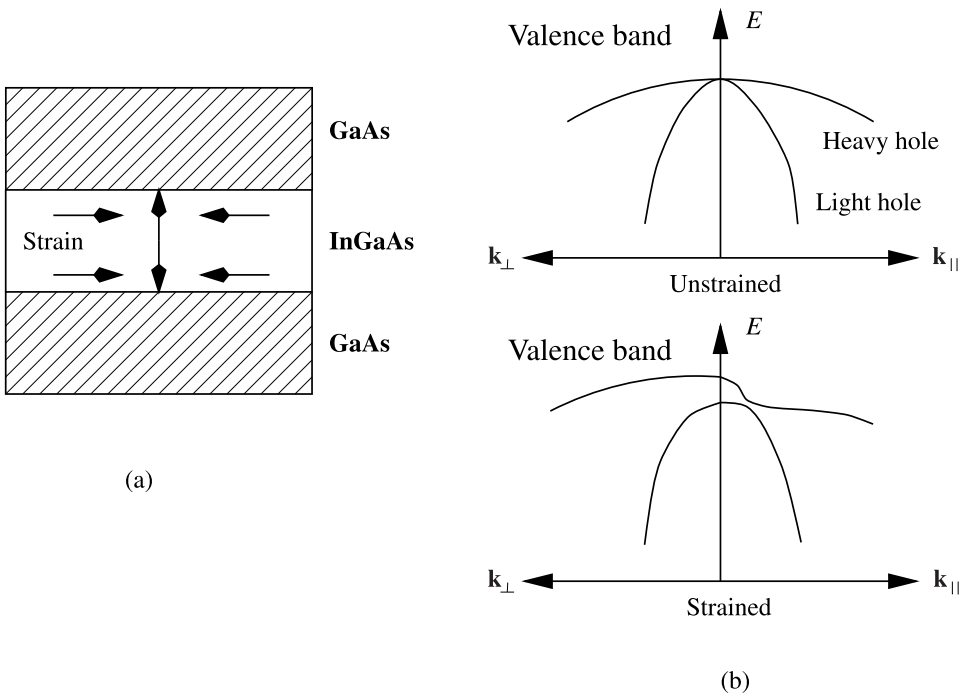

Fig. 1.5. Effect of strain on the band structure of an InGaAs layer grown on the (100) surface of GaAs. The arrows in (a) indicate the direction of the lateral compressive strain and the resulting tensile perpendicular strain. The heavy-hole band structure shown in (b) has shifted upward for transverse wave-vectors and downward for longitudinal wave-vectors resulting in a smaller longitudinal effective mass.

diodes (RTDs). Furthermore, since modern growth techniques can be used to grow semiconductor structures with dimensions as small as a few lattice parameters, new devices making use of the quantum properties of electrons are possible. Among these are quantum wells (applications include laser diodes, HFETs, light switches and so on), superlattices, and RTDs.

Since so many types of semiconductor materials can be grown epitaxially together, it is natural that researchers continuously investigate new materials for the improvement of devices such as HEMTs (High-Electron-Mobility Transistors), HBTs, and RTDs as well as means for further improving the growth techniques. The $Al_xGa_{1-x}As$ system was one of the first material systems used to fabricate HEMTs, HBTs, and RTDs due to its advantageous flexibility when growing lattice-matched structures on the readily available GaAs substrate.

The $In_xGa_{1-x}As/In_xAl_{1-x}As$ system has been subsequently investigated on both InP and GaAs substrates. As we shall see one of its advantages is that it provides a higher electron concentration and is not afflicted by DX (deep trap) center problems for In mole fractions below 60%.

The $Si_{1-x}Ge_x$ system also permits the fabrication of HEMTs, HBTs, RTDs and RITDs (Resonant Interband Tunneling Diodes). It has the advantage of being more easily integrated with other silicon processes. The reader is referred to [5] for a review of its performance achievements and future potentials.

The $Al_xGa_{1-x}N/Al_xAl_{1-x}N$ system has recently attracted a lot of interest. These materials are based on the binaries InN, GaN, and AlN which have large direct (Γ) bandgaps of 1.9, 3.4 and 6.2 eV, respectively. These wide-bandgap materials find application in the creation of green, blue, and violet lasers. This material system is also being investigated for use in high-power microwave electronic devices. High-temperature electronics is also being pursued with this material system and others such as SiGeC. A more complete review of materials and their impact on HBT and HEMT performance is given in Chapters 14 and 19.

1.2.4 Limitations and applications of modern growth techniques

MBE provides the means to grow high-quality materials, with an excellent control of material composition and of epitaxial layer thickness. MBE materials suffer, however, from morphological defects which can affect the smoothness of the semiconductor wafer and the yields. In addition, MBE is an expensive growth technique and other growth techniques such as metal organic chemical vapor deposition (MOCVD) are usually used for high-volume production. However, both MBE and MOCVD have been used in a production environment for the growth of the low-cost laser diodes found in the compact disk recorder and for discrete high-speed HEMT and HBT devices.

MBE and MOCVD technologies are presently the only viable approaches to developing semiconductor transistors which operate at millimeter wavelengths. However, the use of MBE for the production of large-scale digital integrated circuits is limited by the integrated circuit yield. MBE and MOCVD technologies are therefore finding mostly low-scale integrated circuit applications, in digital and analog circuits such as pre-scalers and A/D converters, and in RF (RFIC) and microwave (MMIC) front-end integrated circuits for wireless applications. Another emerging area in which MBE and MOCVD technology will have an important impact is the field of OptoElectronics Integrated Circuits (OEIC). Fiber optics present unrivaled potential for high-speed communication with gigabit bandwidths. Presently this potential is exploited only in expensive communication systems. The development of low-cost OEICs and their integration with the present Si technology will multiply the use of optical local area networks. Applications include the optical wiring of computers, cars, airplanes and so on.

1.3 Crystal and reciprocal lattices

Before discussing heterostructure physics and devices, let us briefly review in this section crystals and reciprocal lattices.

1.3.1 Crystals and lattices

The semiconductor materials used for making devices are in a crystalline state of matter. So a brief review of some of the techniques used for the characterization of crystals is in order.

Crystal structures are defined in terms of a lattice and a basis. The semiconductors we shall consider in this book have either a zinc-blende and or a diamond crystal structure which is realized with a face-centered cubic (fcc) lattice and a basis consisting of two atoms.

The three-dimensional lattice consists of all the points generated by the lattice vectors

$$\mathbf{R} = n_1\mathbf{a}_1 + n_2\mathbf{a}_2 + n_3\mathbf{a}_3, \tag{1.1}$$

where n_1, n_2, and n_3 are integers and where a_1, a_2 and a_3 are the lattice translation vectors.

For a fcc lattice the lattice vector $\mathbf{R}$ is given in the orthonormal coordinates of the Bravais cell (a cube whose side is the lattice parameter a, see Figure 1.6(a) by

$$\mathbf{R} = \frac{a}{2}\begin{bmatrix} 0 & 1 & 1 \\ 1 & 0 & 1 \\ 1 & 1 & 0 \end{bmatrix}\begin{bmatrix} n_1 \\ n_2 \\ n_3 \end{bmatrix}, \tag{1.2}$$

where the lattice translation vectors $\mathbf{a}_1$, $\mathbf{a}_2$ and $\mathbf{a}_3$ for the fcc crystal are defined in Figure 1.6(a).

The fact that fcc or body-centered (bcc) lattices are referred to as cubic lattices (Figure 1.6) is not due to the cubic appearance of their Bravais cell but rather to the fact that an fcc or bcc crystal is left invariant under the 48 symmetries of the O_h (or m3m) group [6] (see Problem 1.2). These 48 symmetries consist of the identity E, inversion I and the rotations of angles $2\pi/2$, $2\pi/3$ and $2\pi/4$ (respectively denoted: C_2, C_3 and C_4) and of their products.

The zinc-blende (or sphalerite) crystal structure of conventional III–V semiconductors is obtained by selecting a basis with two atoms as shown in Figure 1.7. such that, for example, for GaAs, the crystal consists of an fcc lattice of Ga and an fcc lattice of As separated by the vector $a/4(\hat{\mathbf{x}} + \hat{\mathbf{y}} + \hat{\mathbf{z}})$. For C, Si, and Ge crystals the same atoms are used for the basis, and the structure is referred to as the diamond structure.

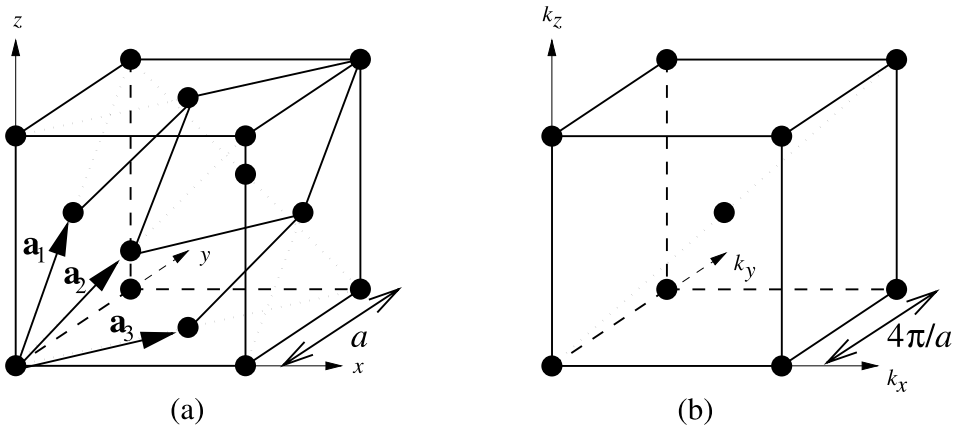

Fig. 1.6. (a) Bravais cell for a face-centered cubic crystal in (direct) space and (b) Bravais cell of the associated body-centered cubic crystal in reciprocal (indirect) space.

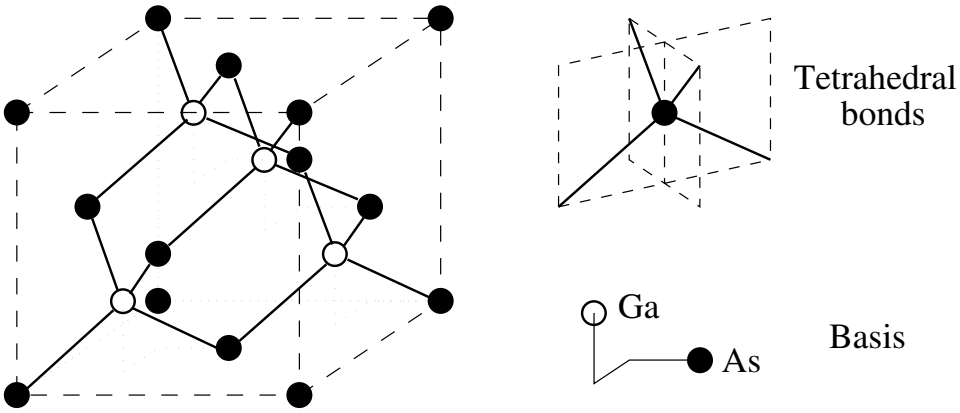

Fig. 1.7. Zinc-blende crystal, its two-atom basis, and the tetrahedral bond structure.

It is interesting to note that the zinc-blende structure does not have an inversion symmetry (I) but is still invariant under the 24 symmetry operations of the T_d subgroup of O_h ($O_h = T_d + I \times T_d$). However, the inversion symmetry is recovered in the band structure due to the time-reversal symmetry of the Schrödinger equation when spin degeneracy is neglected.

1.3.2 The reciprocal lattice

A lattice is a periodic structure in three dimensions. As a consequence, any local physical property of the crystal $f(\mathbf{r})$ is invariant under a translation by a lattice vector $\mathbf{R}$:

$$f(\mathbf{r}) = f(\mathbf{r} + \mathbf{R}). \tag{1.3}$$

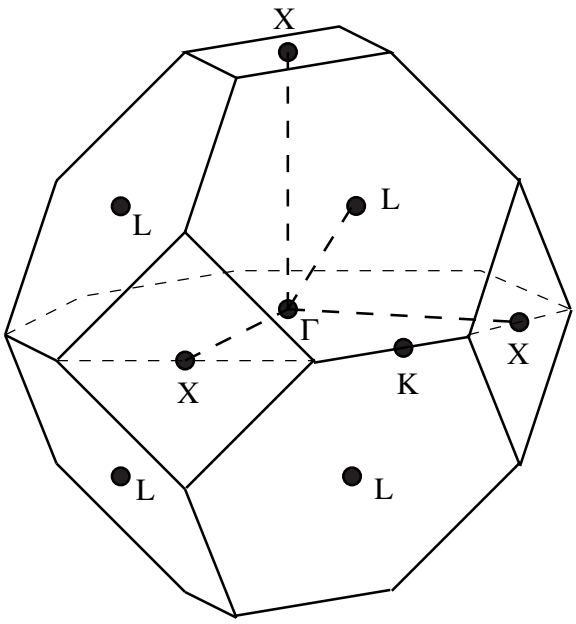

Fig. 1.8. Brillouin zone for the zinc-blende reciprocal lattice.

As $f(\mathbf{r})$ is periodic we can expand it using a Fourier series.

$$f(\mathbf{r}) = \sum_{\mathbf{K}} A_{\mathbf{K}} \exp(i\mathbf{K} \cdot \mathbf{r}),$$

where $\mathbf{K}$ is the so-called reciprocal-lattice vector and $A_{\mathbf{K}}$ the Fourier coefficient.

Now using the translation property we have

$$f(\mathbf{r} + \mathbf{R}) = \sum_{\mathbf{K}} A_{\mathbf{K}} \exp[i\mathbf{K} \cdot (\mathbf{r} + \mathbf{R})] = f(\mathbf{r}).$$

Therefore we must have $\exp(i\mathbf{K} \cdot \mathbf{R}) = 1$ such that the reciprocal-lattice vectors verify

$$\mathbf{K} \cdot \mathbf{R} = n \times 2\pi$$

with n an integer.

For the fcc lattice the reciprocal-lattice vectors $\mathbf{K}$ satisfying this relation are given in the orthonormal coordinates of the Bravais cell by

$$\mathbf{K} = \frac{2\pi}{a} \begin{bmatrix} -1 & 1 & 1 \\ 1 & -1 & 1 \\ 1 & 1 & -1 \end{bmatrix} \begin{bmatrix} m_1 \\ m_2 \\ m_3 \end{bmatrix}, \tag{1.4}$$

where m_1, m_2, and m_3 are integers.

An inspection of $\mathbf{K}$ for the fcc lattice (in direct space) reveals that the reciprocal lattice (in indirect space) is a bcc lattice (see Figure 1.6). The Brillouin zone (the